SANDIA REPORT

SAND97-2295 • UC-704
Unlimited Release
Printed September 1997

Evaluation of Field Enforced Antiferroelectric to Ferroelectric Phase Transition Dielectrics and Relaxor Ferroelectrics for Pulse Discharge Capacitors

B. D. Hoover, B. A. Tuttle, W. R. Olson, D. M. Goy, R. A. Brooks, C. F. King

Prepared by
Sandia National Laboratories
Albuquerque, New Mexico 87185 and Livermore, California 94550

Sandia is a multiprogram laboratory operated by Sandia Corporation, a Lockheed Martin Company, for the United States Department of Energy under Contract DE-AC04-94AL85000.

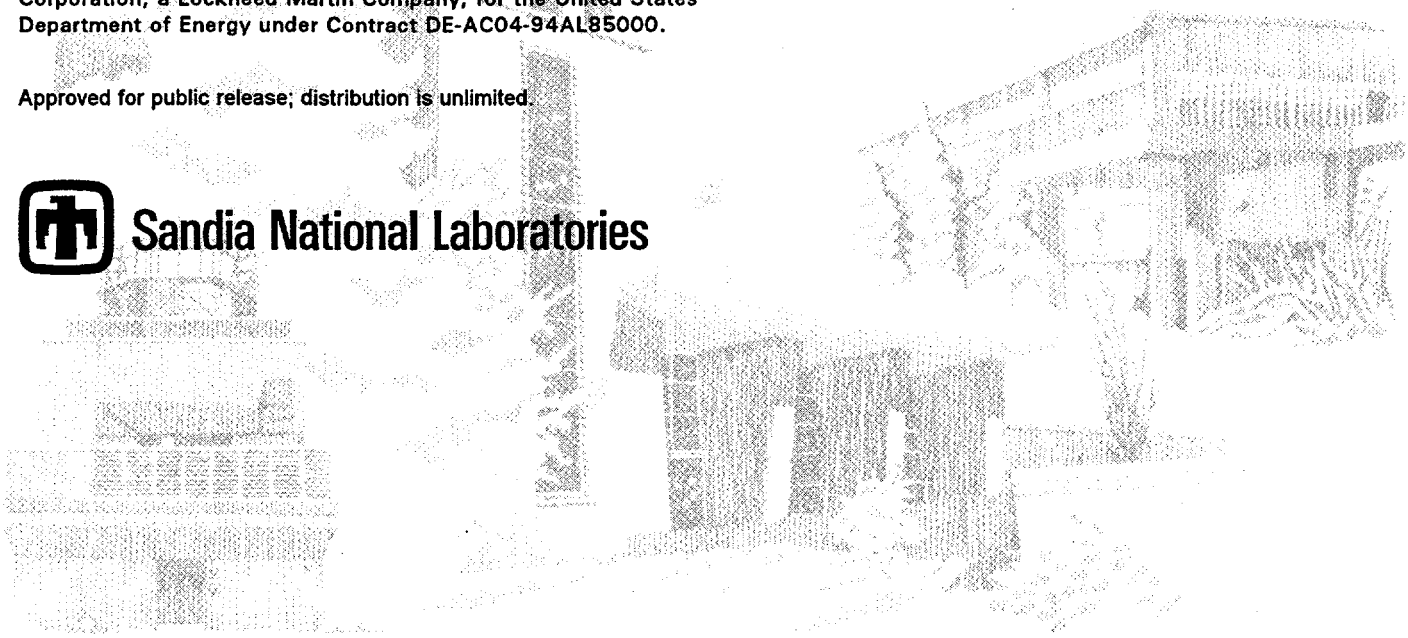

Sandia National Laboratories

Issued by Sandia National Laboratories, operated for the United States Department of Energy by Sandia Corporation.

Available to DOE and DOE contractors from
Office of Scientific and Technical Information
P.O. Box 62
Oak Ridge, TN 37831

Prices available from (615) 576-8401, FTS 626-8401

Available to the public from
National Technical Information Service
U.S. Department of Commerce
5285 Port Royal Rd
Springfield, VA 22161

NTIS price codes
Printed copy: A03
Microfiche copy: A01

SAND97-2295
Unlimited Release
Printed September 1977

Distribution
Category UC-704

EVALUATION OF FIELD ENFORCED ANTIFERROELECTRIC TO FERROELECTRIC PHASE TRANSITION DIELECTRICS AND RELAXOR FERROELECTRICS FOR PULSE DISCHARGE CAPACITORS

B.D. Hoover, B.A. Tuttle andW.R. Olson,
Electronic and Optical Materials Department

D.M. Goy,
Ceramic & Glass Processing Department

R. A. Brooks and C.F. King
Custom Magnetics/Capacitors/Interconnections Department

Sandia National Laboratories
P.O. Box 5800
Albuquerque, NM 87185

Abstract

Discharge capacitors were designed based on materials with antiferroelectric(AFE) to ferroelectric (FE) field enforced transitions that had 10 times the capacitance of relaxor ferroelectrics or state of the art $BaTiO_3$ materials in the voltage range of interest. Nonlinear RLC circuit analysis was used to show that the AFE to FE materials have potentially more than 2 times the peak discharge current density capability of the $BaTiO_3$ or lead magnesium niobate (PMN) based relaxor materials. Both lead lanthanum zirconium tin titanate (PLZST) AFE to FE field enforced phase transition materials and PMN based relaxor materials were fabricated and characterized for Sandia's pulse discharge capacitor applications. An outstanding feature of the PLZST materials is that there are high field regimes where the dielectric constant increases substantially, by a factor of 20 or more, with applied field. Specifically, these materials have a low field dielectric constant of 1000, but an effective dielectric constant of 23,000 in the electric field range corresponding to the FE to AFE transition during discharge. Lead magnesium niobate (PMN) based relaxor materials were also investigated in this project because of their high dielectric constants. While the PMN based ceramics had a low field dielectric constant of 25,000, at a field corresponding to half the charging voltage, approximately 13 kV/cm, the dielectric constant decreases to approximately 7,500.

Acknowledgments

The authors would like to acknowledge the assistance of Gary Zender and Alice Kilgo in the microstructural analysis of specimens. In addition, Mike Eatough provided accurate lattice parameter measurements for theoretical density calculations. Further, the technical input of Dave Zamora on adhesive bonding and Augie Chapa on packaging were very much appreciated. Pat Smith provided program support and led numerous technical discussions with regard to pulse measurements and volume requirements. Discussion of circuit analysis with Roger Edwards was enlightening and his computer program was frequently used to determine the equivalent capacitance for pulse discharge measurements.

Contents

page

Acknowledgments 2

Introduction.....5

RLC Circuit Analysis.....7

Dielectric Constant Approximation From Polarization Versus Field Behavior.....10

Materials Processing.....14

Electrical Properties of PLZST Ceramics.....18

Summary.....24

References.....24

Figures

1 Schematic Diagram of RLC Circuit.....7

2 Discharge Current Waveforms for Linear RLC Elements for Different Values of Resistance for a Series Connected 105 nF Capacitor and 18 nH Inductor.....8

3 Discharge Current Waveforms for Linear RLC Elements for Different Values of Inductance for a Series Connected 105 nF Capacitor and a .289Ω Resistor.....8

4 Discharge Current Waveforms for Linear RLC Elements for Different Values of Capacitance for a Series Connected 0.289 ohm Resistor and a 18 nH Inductor..... 9

5 Peak Discharge Current Versus Capacitance for 0.25 ohm Resistor and 40 nH Inductor Circuit Elements.....10

6 Dielectric Constant Versus Applied Electric Field for 0.025 cm, 0.038 cm, and 0.050 cm (10, 15 and 20 mil) Thick PMN Dielectrics.....11

7 Dielectric Constant Versus Applied Electric Field for Both Bias Measurements and for dP/dE Calculations.....12

8 Schematic Drawing of a Polarization Versus Field Hysteresis Characteristic Showing Path of FE to AFE Transition During Discharge.....13

9 Diagram Showing Alumina Crucible Configuration for Firing PLZST Ceramics.....14

10 SEM Micrograph Showing Grain Size Distribution of PLZST 60/30/10 Ceramic Fired at 1300°C for 6 hours.....16

11 SEM Micrograph Showing Grain Boundary Regions and Subgrain Structure of PLZST 60/30/10 Ceramic Fired at 1300°C for 6 Hours.....16

12 Phase Diagram for PLZST.[5].....18

13 Dielectric Constant Versus Applied Electric Field for PMN for 0.038 cm, and 0.050 cm (15 and 20 mil) Thick Samples and for PLZST 2/60/29/11 AFE-FE Material. Effective Dielectric Constants Corresponding to Linear Capacitance Approximation of Pulse Discharge Current Measurements are Indicated.....19

14 Pulse Discharge Current Versus Time for).015" Thick PMN Capacitor Charged to 1000 Volts.....20

15 Capacitance Versus Voltage for 0.038 cm (15 mil) Thick PMN and PLZST 2/60/31/9 Ceramics.....21

16 Polarization Versus Field Characteristics for PLZST 2/60/31/9 at the Following Temperatures: (a) 25°C, (b) 5°C, (c) 0°C, (d) -10°C (e) -25°C, (f) -35°C, (g) -45°C and (h) -60°C.....22

17 Polarization Versus Field Hysteresis Loop for PLZST 2/60/31/9 with 120 kV/cm Applied Field.....23

Tables

1 Discharge Energy Densities for High Dielectric Constant Materials.....5

2 Weight Loss and Density of PLZST Ceramics.....15

3 Theoretical Densities for PLZST Ceramics.....15

4 Polarization and Electric Field Data For PLZST Ceramics as a Function of Sn/Ti Ratio.....19

INTRODUCTION

The goal of this project was to evaluate two different dielectric materials technologies for high peak current (greater than 1000 amperes) pulse discharge capacitors. These two technologies were: (1) field enforced AFE to FE PLZST materials and (2) PMN based dielectrics. Both technologies offer promise of greater than 1000 ampere discharge in the 30 to 70 nanosecond time frame from a small volume (0.25 cm^3 or less) capacitor. High dielectric constant PMN capacitors have recently been developed for Sandia pulse discharge capacitor applications [1,2]. The present work compares the PMN technology to AFE to FE PLZST technology and provides a more detailed analysis of the PMN capacitor discharge behavior. A more rigorous RLC circuit analysis is also presented in this report. Dielectric constants measured at half the charging field bias (approximately 13 kV/cm) are shown to provide a good approximation for the peak pulse discharge current. While the AFE to FE PLZST ceramics can be tailored by chemical composition and microstructure to have a high effective dielectric constant of approximately 10,000 at this field, the PMN based dielectrics have a lower dielectric constant of about 7,500 at these fields, using polarization vs. field derivative calculations. Compared to most other materials, a dielectric constant of 7,500 is still very high.

Table 1. Discharge Energy Densities For High Dielectric Constant Materials

Material	Energy Density (J/cm^3)	Field (kV/cm)	Authors
$BaTiO_3$	1.34	333	G. Love
PMN	0.64	40	B. Tuttle
$BaTiO_3$	1.1 2.0	160 330	W. Huebner
$P(Hf,Ti)O_3$	4.0	200	M. Waugh, C. Randall
PLZT	5 to 10	N/A	G. Haertling
PLZST	3.5	120	K. Merkowski, L.Cross
PLZST	3	120	B.Hoover

Energy density is a metric that is often used to compare different capacitor materials, especially for applications for which overall volume is important. However for pulse discharge capacitor detonator applications, the peak current and peak power over a critical interval of time is a more relevant figure of merit than total energy density. We have shown that this peak power is dependent in highly volumetric efficient capacitor systems on the dielectric constant behavior at high fields, specifically fields corresponding to approximately half the initial charging voltage. Nonetheless, we briefly review the energy densities of our two technologies versus that determined by other workers (Table 1). The energy density that our PMN capacitors designed for the Highly Integrated Detonator System (HIDS) application [1,2] is subjected to is approximately 0.14 J/cm^3. The capacitor is a single layer PMN dielectric that is 0.038 cm (0.015") thick and is charged to

1000 volts. The highest energy density that was obtained for these PMN ceramics developed in the report by Tuttle and coworkers [2] was 0.64 J/cm^3 at 2000V. Waugh, Randall and coworkers [3] have shown energy densities of approximately 4 J/cm^3 for field enforced AFE to FE lead hafnate /lead titanate based capacitors for which 200 kV/cm was applied. Haertling [4] has claimed energy densities of 5 to 10 J/cm^3 for AFE to FE PLZT materials. Recently, Merkowski, Cross and coworkers [5] have shown that hot isostatically pressed PLZST ceramics can withstand fields of up to 120 kV/cm and that the calculated energy storage capability is approximately 3.5 J/cm^3. We have fabricated PLZST 60/31/9 ceramics in this study that withstood 120 kV/cm and had calculated energy storage densities of 3 J/cm^3. For comparison, the very best barium titanate dielectrics that were evaluated in the article by Love [6] have energy densities of 1.34 J/cm^3 for 333 kV/cm applied field. Thus, for high energy density discharge applications, field enforced AFE to FE dielectrics appear very attractive.

RLC CIRCUIT ANALYSIS

Discharge currents of an RLC circuit can be either overdamped, critically damped or under damped (Figure 1). If the resistance in the circuit is less than a critical resistance, defined as the square root of the inductance divided by the square root of the capacitance, then the circuit is underdamped. If the resistance is equal to the critical resistance, then the circuit is critically damped, and if the resistance is greater than the critical resistance the circuit is overdamped. A schematic diagram of a basic series RLC network is shown below.

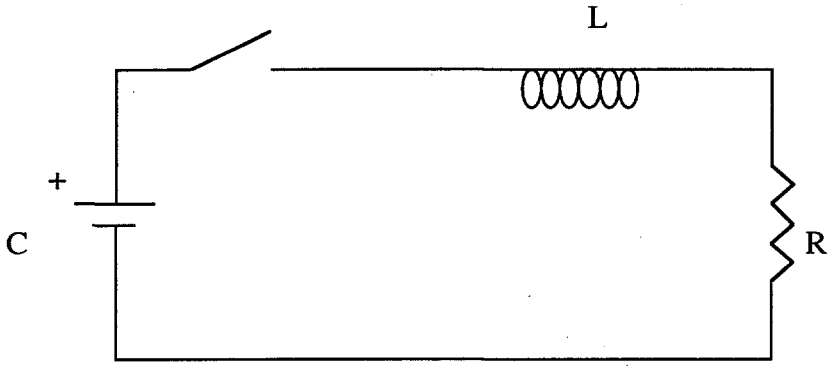

Figure 1. Schematic Diagram of RLC Circuit.

Underdamped RLC circuits directly apply to the majority of the pulse discharge testing in this report. For underdamped conditions, RLC circuits containing linear capacitors were studied to obtain a better understanding of how changes in the capacitance, inductance and resistance affect peak current output. The function that describes the discharge current in terms of the resistance, inductance and capacitance is a sinusoidal function that is modified by a constant and an exponential decay function. The equation is as follows:

$$i(t)=V_0 \div[\mathrm{sqrt}(L/C-R^2/4)]*\exp(-Rt/2L)*\sin[\mathrm{sqrt}(1/LC-R^2/4L^2)*t] \qquad (1)$$

The effects of the change in capacitance were most emphasized in our studies for two reasons:

(1) the inductance and resistance will typically be constants and be determined by the specifications of the particular fireset and
(2) our work was devoted to fabrication and characterization of new capacitor materials.

However, both engineers and scientists need to be aware that small changes in resistance and inductance loads have a large effect on the peak pulse current . The effects of the changes in resistance, inductance and capacitance on peak current for a RLC discharge circuit are shown in Figures 2, 3, and 4, respectively, while other circuit parameters are held constant.

Assuming a linear inductor and a linear capacitor connected in series, lower load resistance results in a higher peak current and a slower decay of the sinusoidal function

with time(Figure 2). Specifically decreasing the resistance from 0.75 ohms to 0.25 ohms,

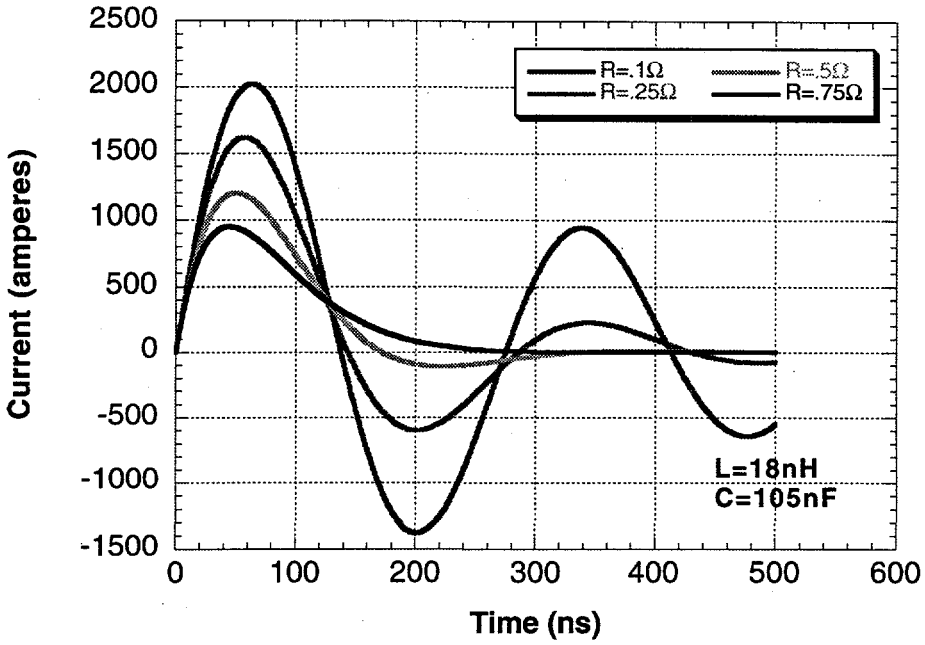

Figure 2. Discharge Current Waveforms for Linear RLC Elements for Different Values of Resistance for a Series Connected 105 nF Capacitor and 18 nH Inductor.

results in a 35% higher peak discharge current. These values mimic changes to our baseline pulse discharge circuit parameters over the course of the last year. For a linear resistor and capacitor connected in series, lowering the series inductance of the RLC discharge circuit caused the peak discharge current to reach a higher amplitude in a shorter

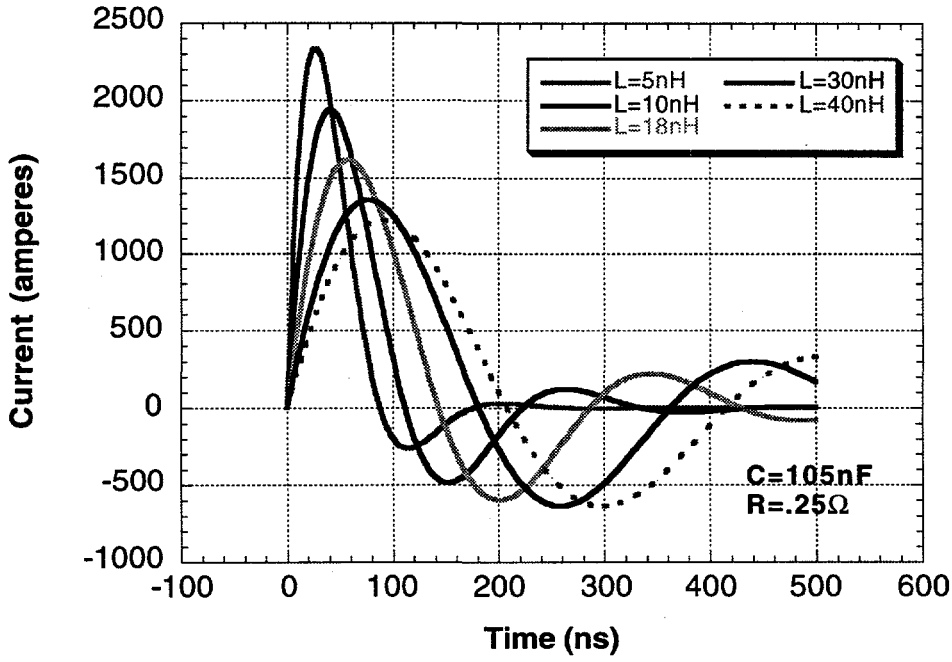

Figure 3. Discharge Current Waveforms for Linear RLC Elements for Different Values of Inductance for a Series Connected 105 nF Capacitor and a .289Ω Resistor.

time (Figure 3) . This is due both to changing the exponential term in equation 1 and to decreasing the period of the sine wave; effectively the decay exponential does not drop as fast with time and the first peak occurs earlier. Specifically decreasing the inductance from 40 nH to 12 nH results in an increase of the pulse discharge current by 60%. These figures allow normalization of a change that has occurred in our baseline test set up over the course of the last year. The baseline resistance and inductance values for our pulse discharge apparatus for evaluating capacitors has changed from having a 40 nH and 0.75 ohm load in series to a 12 nH and 0.25 ohm series load.

As capacitance increases for a given resistive and inductive load, the peak current substantially increases, see Figure 4. A capacitance of 40 nF corresponds to the capacitance

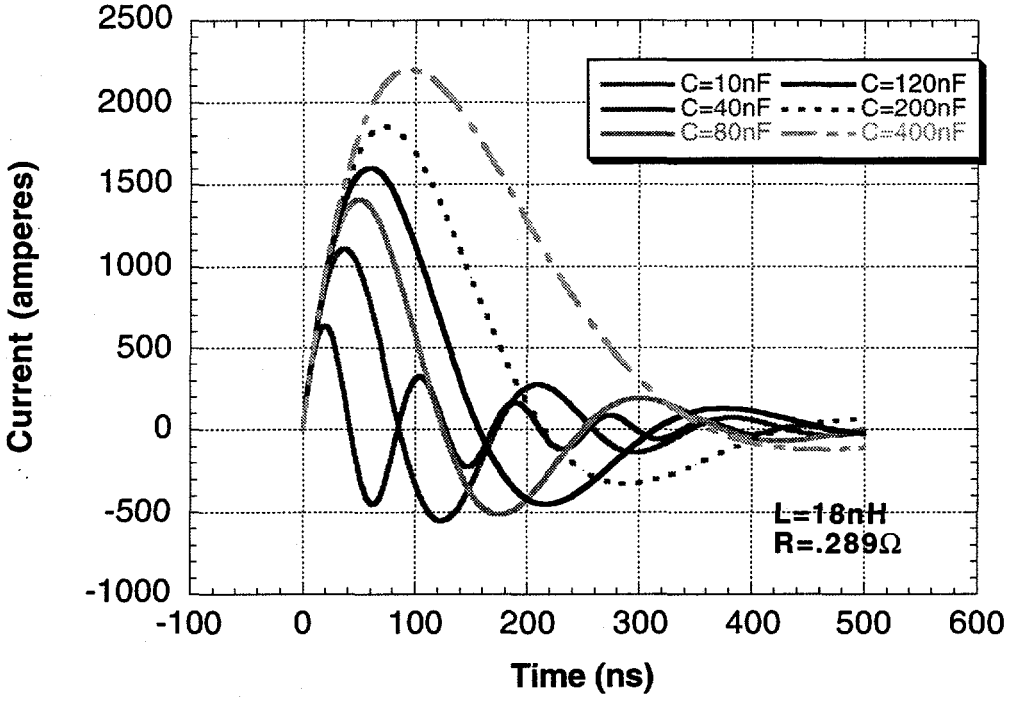

Figure 4. Discharge Current Waveforms for Linear RLC Elements for Different Values of Capacitance for a Series Connected 0.289 ohm Resistor and a 18 nH Inductor

of the PMN capacitor at the charging voltage of 1000 volts. If the capacitance is doubled to 80 nF, which corresponds to the capacitance of the PMN capacitor at 500 volts, the peak current increases by approximately 30%. If the capacitance increases to 200 nF, a value which is projected under ideal conditions for the single layer AFE to FE material, then the peak discharge current nearly doubles.

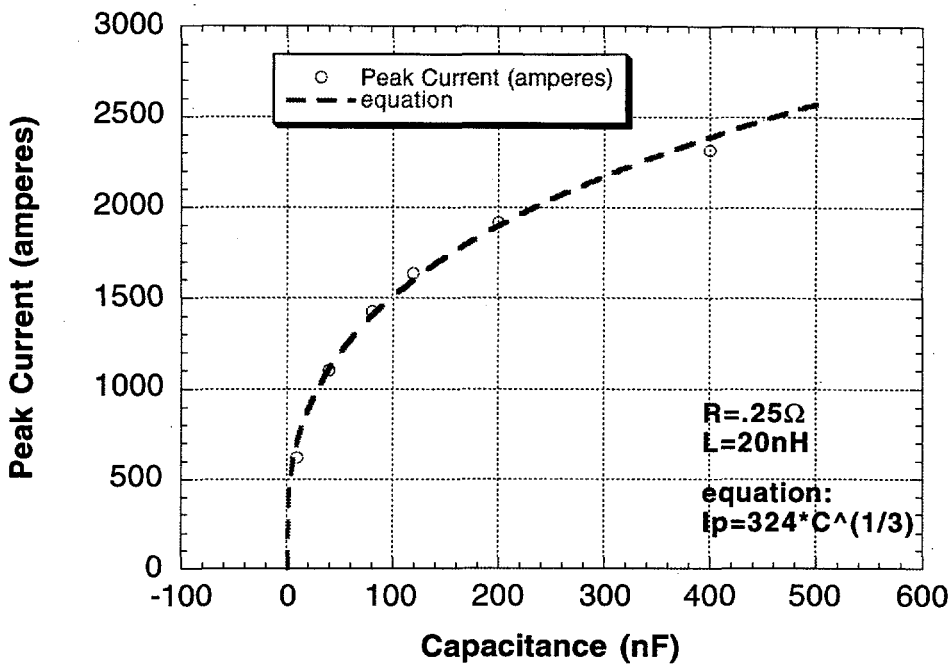

Figure 5. Peak Discharge Current Versus Capacitance for 0.25 ohm Resistor and 40 nH Inductor Circuit Elements.

The change in the peak discharge current is plotted as a function of capacitance in Figure 5. Further, this data was fit by the following equation with confidence limits of .99489 which defined the change of peak discharge current with capacitance. The equation describing the peak discharge current - capacitance relationship is:

$$Ip = 324*C^{1/3} \qquad (2)$$

There has been some question in the past as to how the current output of an under damped RLC circuit is affected by a change in the discharge capacitor. From equation 1, we have calculated that the current amplitude during the initial discharge current increase is proportional to the square root of the capacitance. However, the peak current output, which is of primary importance for fireset applications, increases as the cube root of capacitance. The reason that peak current is less strongly influenced by capacitance is that the peak currents occur at increasing time with the increase of capacitance. This is due to an increased period of the sine function with increasing capacitance. The decaying exponential term causes the peak current at longer time periods to be less than that calculated based solely on the amplitude portion of equation (1) which is proportional to the square root of capacitance. The $C^{1/3}$ dependence of peak current for this given capacitance range is strictly empirical, for larger values of capacitance the peak current will have an even weaker capacitance dependence. Thus, to fully exploit large capacitors, design engineers must lower the inductance so that the effect of the exponential decay factor is minimized. We have used these concepts of linear modeling to *a priori* approximate nanosecond time frame, peak pulse discharge currents for different PMN based capacitors.

Dielectric Constant Approximation from Polarization vs. Field Behavior

The RT66A ferroelectric tester was used to generate polarization versus field data. Because the dielectric constant is the change in polarization divided by the change in field ($\Delta P/\Delta E$) times the reciprocal permittivity of free space ($1/\varepsilon_0$),

$$k=(\Delta P/\Delta E)*(1/\varepsilon_0) \qquad (3)$$

we used the derivative of the polarization versus electric field hysteresis loops to calculate the behavior of the dielectric constant versus field. Digitized polarization vs. electric field characteristics were approximated by a power series expansion using computer software (Kaleidagraph). The derivative of the power series function was then calculated, plotted, and then evaluated at the desired field level to obtain the dielectric constant in equation (3). Capacitance versus voltage for the PMN material was then calculated for various voltages using equation 4,

$$C(V) = k(V) *A*\varepsilon_0/T \qquad (4)$$

where A is area and T is thickness. Figure 6 is a graph of the dielectric constant versus applied field (using equation 3) for PMN dielectrics of three different thickness values that were evaluated in the HIDS program. For fields greater than 5 kV/cm, the dielectric constant was almost the same for all of the PMN samples, implying that interfacial effects had minimal impact at field levels of interest for pulse discharge applications.

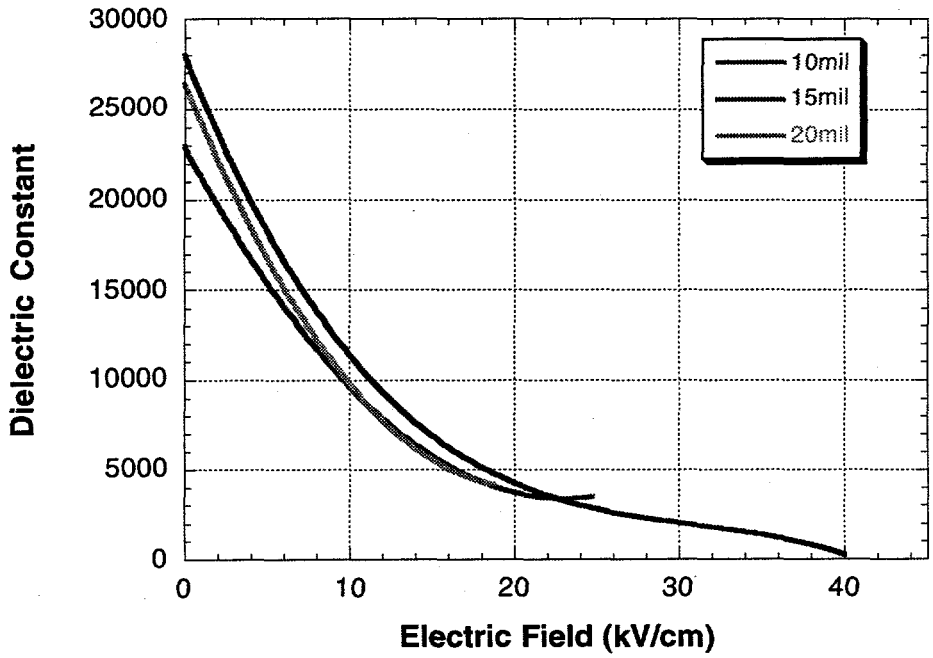

Figure 6. Dielectric Constant Versus Applied Electric Field for 0.025 cm, 0.038 cm, and 0.050 cm (10, 15 and 20 mil) Thick PMN Dielectrics

The PMN capacitor that has been used in the HIDS prototype is a slim loop ferroelectric with extremely high dielectric constant. The current versus time characteristic obtained from pulse discharge measurements was modeled using linear RLC circuit elements. The fit using the linear RLC analysis computer program designed by Roger Edwards (Dept. 1251) was surprisingly good. The term surprisingly is used since the PMN dielectrics are highly nonlinear, that is, their dielectric constant changes substantially with field. An advantage of the good fit with the linear circuit element program is that a specific field range of measurement for capacitance that relates most strongly to the pulse discharge test could be determined. A semiquantitative model of the discharge current pulse of these capacitors was obtained from the capacitance - voltage measurements and indicated which capacitors had the highest current output. A precise quantitative model generated by inserting the capacitance function obtained from the hysteresis measurements into the current equation has not been obtained because the capacitance is in terms of voltage and the voltage change in terms of time is still unknown. Another issue is that the present curve fit program was designed for linear capacitors and that it compensates for the changing capacitance by adjusting the inductance and resistance when they are actually constant. Modifying the program for nonlinear circuit elements was beyond the scope of this program. Reasonable semiquantitative fit with the linear RLC model did permit selection of capacitors for pulse discharge tests by capacitance-voltage measurements.

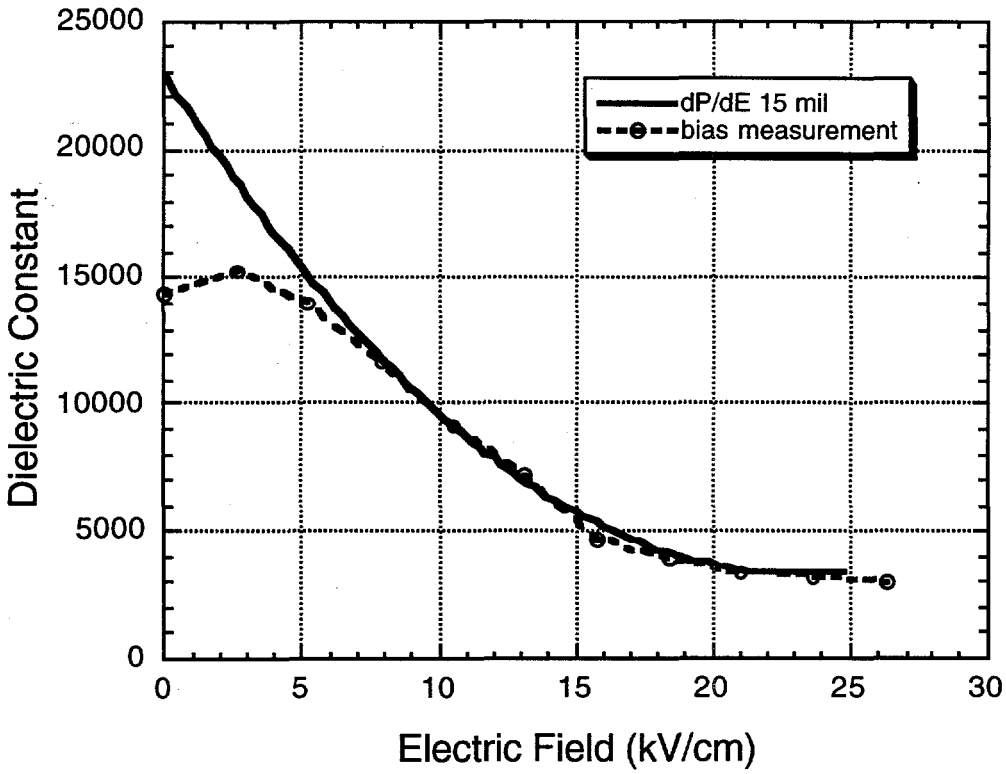

Figure 7. Dielectric Constant Versus Applied Electric Field for Both Bias Measurements and for dP/dE Calculations.

Modeling using linear circuit elements was done to calculate the ideal field to apply to the sample, and in turn, to determine the appropriate thickness to optimize current output. It is recognized that the frequency for the dielectric constant in the pulse discharge test (50 ns or 20 MHz) is considerably different than that of the hysteresis measurement (1.1ms or 900 Hz). However, the dielectric dispersion over this frequency range affects our results only

slightly. We used small signal (1 kHz) capacitance versus dc bias field data to check the accuracy of the dP/dE measurements and the results are in shown in Figure 7. The two plots agree quite well at higher fields. High field capacitance is more germane to pulse discharge output than low field capacitance where agreement is not as good.

We used the capacitance versus voltage technique developed for the PMN capacitors to select appropriate compositions for AFE to FE PLZST discharge capacitors. Capacitance measured at 440 volts by either technique was similar to that produced by the linear capacitor approximation from the pulse discharge modeling conditions for the 15 mil PMN sample. A .289Ω at 18 nH series inductance load was used. From this data we were able to determine that a highly desirable dielectric characteristic was one that had a large dielectric constant in the 10 to 20 kV/cm range. A material that has a FE to AFE transition with decreasing field between 10 and 20 kV/cm should meet the above criteria. Figure 8 is a schematic diagram of a dielectric hysteresis loop for an AFE-FE material. The path that is most important is shown by path B in the figure which shows the polarization change as the capacitor discharges.

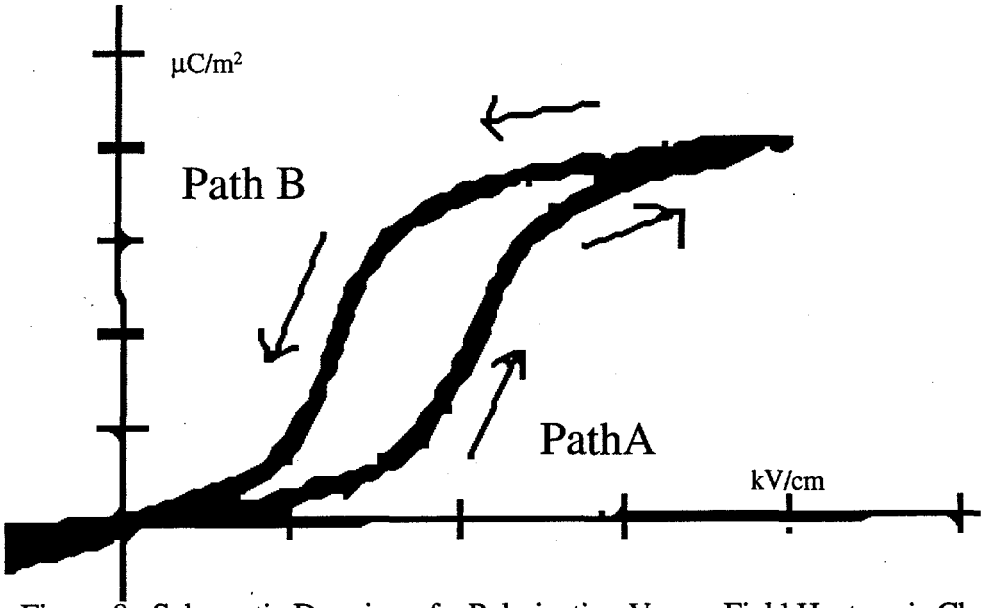

Figure 8. Schematic Drawing of a Polarization Versus Field Hysteresis Characteristic Showing Path of FE to AFE Transition During Discharge.

Materials Processing

The PLZST AFE-FE field enforced materials were made using reagent grade PbO(Acros, NJ), La_2O_3 (Acros, NJ), ZrO_2(TAM, NY), TiO_2(Acros, NJ) and SnO_2(Harshaw,) powders. First, the precursor powders were dried for at least 10 hours at 100°C. All of the powders were then weighed out to .005g of the calculated weight using an analytical balance, with a total batch weight of 100g. A b-site cation vacancy model was used to calculate the formula weight and the weight of individual constituents[8]. The powders were placed in a 500 mL polyethylene jar with 400g of 10 x 10 mm zirconia grinding media and 100 mL of optical grade ethanol, and then ball milled for 2 hours. After milling, the ethanol and powder slurry was poured into a pyrex drying dish and dried at 50°C for 12 hours. The PLZST powders were then removed from the glassware and calcined in an alumina crucible at 875°C for 4 and then dry ball milled with zirconia media for 2 hours. This produced, to the eye, a relatively homogeneous mixture of the precursor powders.

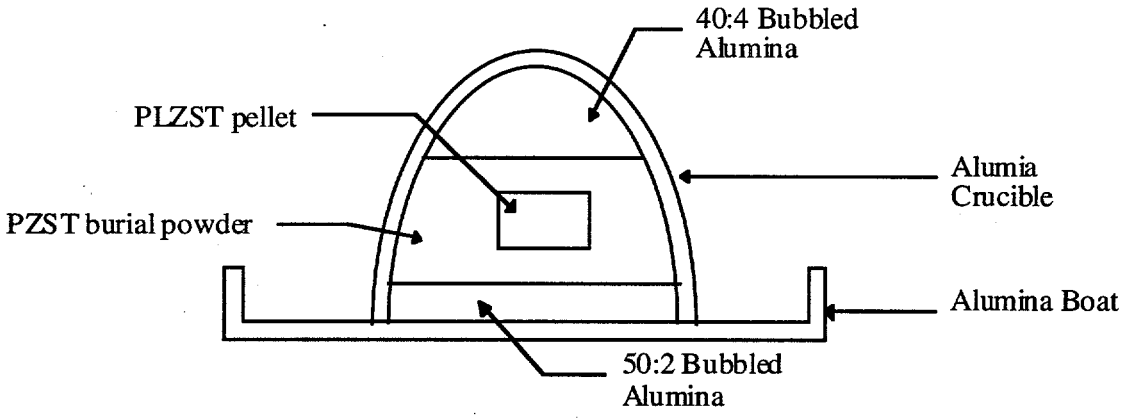

*40:4 Bubbled Alumina is a mixture of hollow alumina spheres ranging from ~.5mm to ~1.5mm with PbO. Alumina: PbO ratio is 40:4

*50:2 Bubbled Alumina is a mixture of hollow alumina spheres ranging from ~.5mm to ~1.5mm with PbO. Alumina: PbO ratio is 50:2

Figure 9. Diagram Showing Alumina Crucible Configuration for Firing PLZST Ceramics.

The powder was uniaxially pressed at 2000 psi for 30 seconds into 3g pellets that were approximately 1.2 cm in diameter and 0.5 cm thick. The pellets were fired at 1300°C for 6 hours in an alumina crucible surrounded by PZST burial powder as shown in Figure 9. The percent theoretical densities measured by both geometric and Archimedes techniques and the percent weight loss are shown in Table 2. For these small 3 gram pellets that were somewhat deformed these densities should be considered a rough approximation. The deformities cause some error in the geometric measurement. Because of the considerable open porosity in some of the specimens, the Archimedes measurement can provide slightly higher densities than are representative of the sample. These are the reasons that there is as much as a 7% difference in density measurements between the two techniques. The weight loss was proportional to the initial PbO content in the samples, with the 3 mol% excess PbO content ceramic having at least twice the weight loss of the samples containing 0 mol%

initial excess Pb content. All materials are approximately 2 weight percent or 3 mol% deficient in PbO compared to ideal stoichiometric values. Improvements in the initial firing configuration should lead to weight loss control at the 0.1 to 0.2 weight percent level.

Table 2. Weight loss and Density of PLZST Ceramics.

Sample	% Theoretical Geometric Density	% Theoretical Density Archimedes	%Weight Loss
PLZST 60/31/9	80.9%	85.1%	1.34%
PLZST 60/30/10	87.9%	87.5%	1.73%
*PLZST 60/29/11	87.3%	94.3%	4.33%

*3mol% , 1.8wt% excess Pb added during powder mixing.

Theoretical densities for the PLZST 29/11 and PLZST 29.5/10.5 ceramics were calculated using the a_0 and c_0 lattice parameters which were obtained using X-ray diffraction from the (002) and (200) d-spacings of the antiferroelectric materials with tetragonal symmetry. The theoretical densities for the other two PLZST ceramics were extrapolated assuming the relationship between composition and theoretical density was linear. The theoretical densities are shown in Table 3.

Table 3. Theoretical Densities for PLZST Ceramics.

Composition (Sn/Ti mol ratio)	31/9	30.5/9.5	30/10	29.5/10.5	29/11
Theoretical Density (g/cm^3)	8.445	8.448	8.451	8.454	8.457

Microstructures of the PLZST 60/30/10 ceramic that had been polished to a 0.05 μm colloidal silica finish and etched with a 600:11:1 deionized water: HF: HCl solution are shown in figures 10 and 11. The grain size of the PLZST 60/30/10 ceramic was 6.6 μm as determined by the linear intercept method using no mulitplicative shape factors. Grains ranged in size from 2 μm to 20 μm. Close examination of Figure 11, indicates relatively clean grain boundaries after etching and the presence of linear 90° type AFE domain structures in larger grains. Further, evidence of trapped intragranular pores was observed for many grains. It is not difficult to believe that many of the pores are connected to the surface of the ceramic, thus resulting in what is termed as open porosity. The Archemides technique when executed properly gives a measure of the closed porosity.

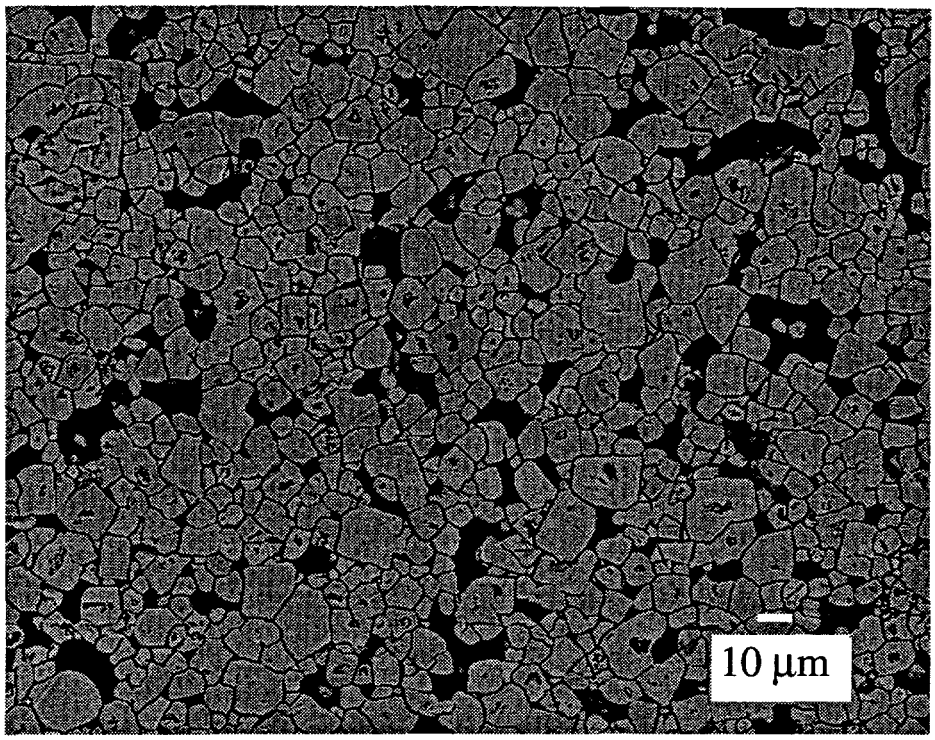

Figure 10. SEM Micrograph Showing Grain Size Distribution of PLZST 60/30/10 Ceramic Fired at 1300°C for 6 hours.

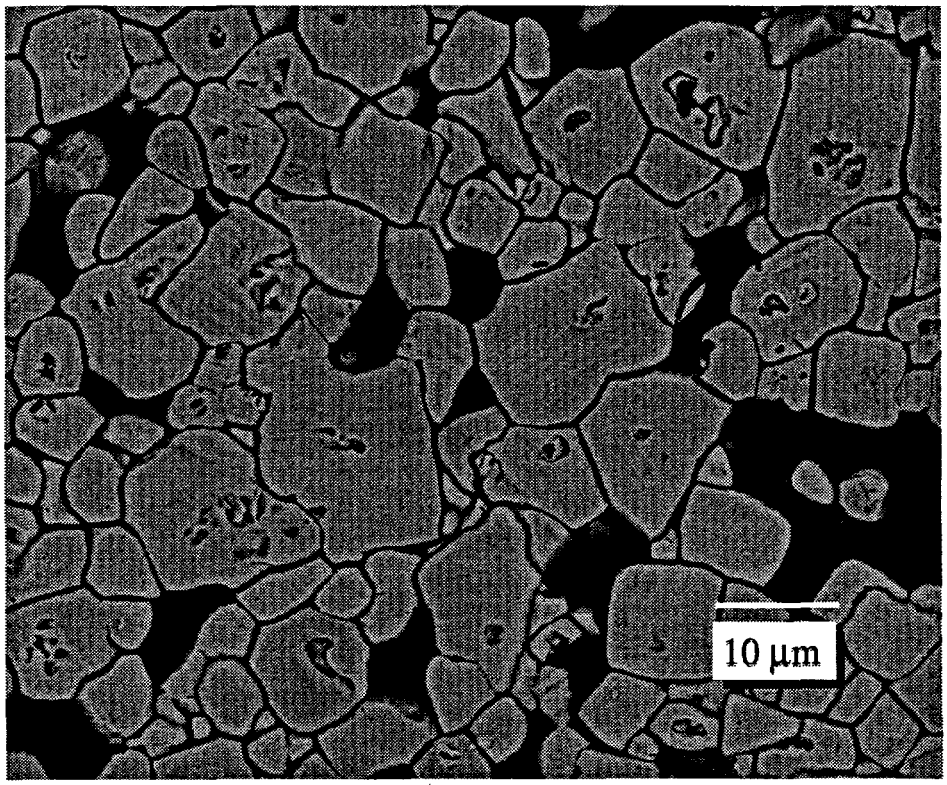

Figure 11. SEM Micrograph Showing Grain Boundary Regions and Subgrain Structure of PLZST 60/30/10 Ceramic Fired at 1300°C for 6 hours.

Samples of 0.038 cm and 0.019 cm (15 and 7.5 mil) thickness for electrical measurements were prepared using a diamond saw. PLZST surfaces were prepared for electroding by grinding with 600 grit silicon carbide paper. The samples were then cleaned using an ultrasonic acetone wash for 2 minutes. They were then annealed at 800°C for 30 minutes to remove any organics and perhaps remove some subsurface damage. Finally, the samples were electroded by sputter deposition of 1000Å gold on top of 200Å chromium on both sides of the sample.

Lead magnesium niobate based ceramics were fabricated by conventional oxide powder processing from commercially available PMN powder (TAM Y5V183U dielectric powder, Product No. 52639, lot 42630; TAM Ceramics, Niagara Falls, NY). The approximate chemical composition of our PMN-based dielectrics was

$$Pb(Mg_{0.33}Nb_{0.67})_{0.94}Ti_{0.06}Cu_{0.06}O_3.$$

The term PMN will be used through out this report for materials of this chemical composition. The powders were intimately mixed with 4 weight percent water as a binder by hand mixing with a glass stirring rod and then placed in covered containers for a minimum of 20 hours. The storage resulted in a reasonably uniform moisture distribution throughout the powders. These powders were uniaxially pressed at 15 ksi and then isostatically pressed at 30 ksi to achieve approximately 60% green densities. Our baseline thermal processing treatment was 1100°C for 3 hours using no atmosphere powder. Fired densities were approximately 96% of theoretical density.

During the course of the project, PMN ceramics that ranged in diameter from 0.5" to 1.07" were fabricated, with 1.07" diameter materials being the baseline. Typically fired PMN bodies were approximately 1" in height. Dielectric layers of the desired thickness, ranging from 0.010" to 0.030", were sliced out of the fired cylinder using a diamond ID saw. The samples were then thermally cleaned using a 760°C/ 4.8 hr anneal with a slow cooling rate (120°C/hr) to room temperature. The thermal clean removed all cleaning solvents and may have minimized subsurface machine damage. Silver electrodes (Dupont 7095 Ag frit paste) were screen printed onto the PMN dielectrics using a 1.04" diameter mask. A thermal treatment of 593°C for 20 min bonded the silver electrode to the PMN dielectric well enough to withstand over 100,000 discharge pulses of approximately 1000 amperes each. The electroded area corresponds to 0.85 in^2 and is the area to which most of our electrical measurements were normalized.

Electrical Properties of PLZST Ceramics

We fabricated a series of PLZST materials for prototype discharge capacitors that were located along a tie line of constant 60 mol% Zr content. All materials contained 2 mol% lanthanum addition. The tin:titanium ratio was modified to fabricate AFE materials that systematically varied in the field that was needed to induce the ferroelectric phase. The location of the compositions fabricated are approximately marked by the circle labeled B2

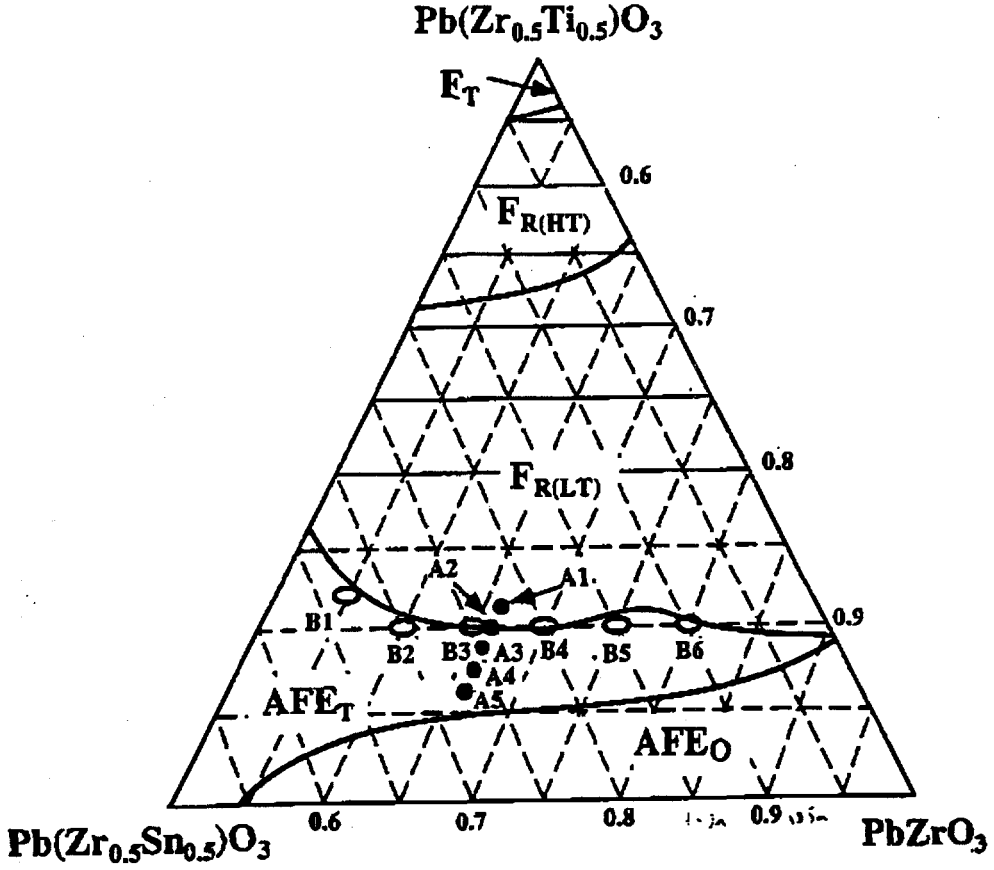

Figure 12. Phase Diagram for PLZST.[5]

on the phase diagram, shown in Figure 12. The PLZST 27/13 composition has an AFE to FE phase transition at 25°C and zero electric field. Increasing the tin to titanium ratio increases the free energy difference between the AFE and FE phases and thus increases the electric field needed to induce the ferroelectric phase. The series of compositions fabricated and the pertinent hysteresis properties are listed in Table 4.

Table 4. Polarization and Electric Field Data For PLZST Ceramics as a Function of Sn/Ti Ratio.

Composition	$E_{AFE\ to\ FE}$	$E_{FE\ to\ AFE}$	Polarization
2/60/31/9	90	70	25
2/60/30/10	60	40	25
2/60/29.5/10.5	45	20	28
2/60/29/10	36	10	30

The polarizations were measured for saturated loops with an applied field approximately 20% larger than the transition field. Initially we fabricated PLZST 2/60/30/10 and PLZST 2/60/31/9 ceramics to determine how the FE-AFE transformation field changed with changing composition. The PLZST 31/9 composition FE-AFE transition occurred at 70kV/cm, while the PLZST 30/10 composition shifted the transition field to 40kV/cm. Assuming a linear change of transition field with chemical composition, the desired response of a 10 kV/cm FE to AFE transition during discharge would occur for a composition of PLZST 29/11. We fabricated two new PLZST ceramics to meet this goal: PLZST 29.5/10.5 and PLZST 29/11. The PLZST 29/11 had a field enforced transition at about 10 kV/cm, and a maximum capacitance at approximately 14.5 kV/cm which was approximately the correct field for the HIDS specifications.

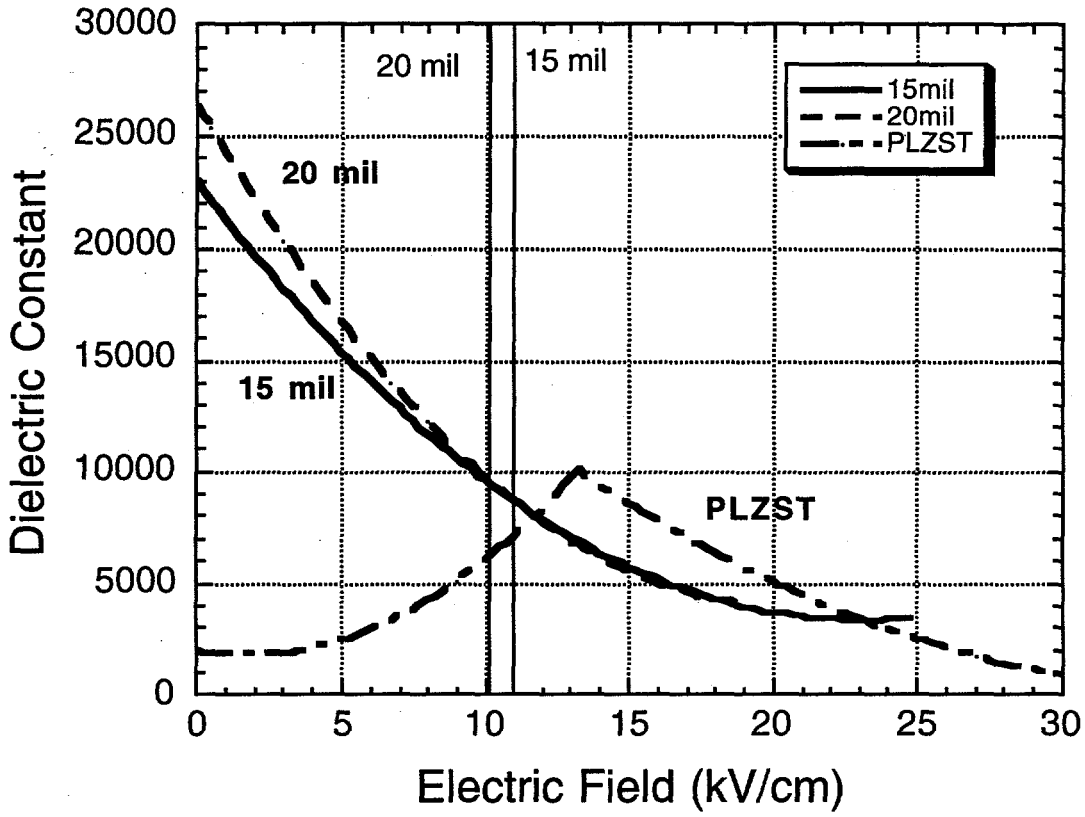

Figure 13. Dielectric Constant Versus Applied Electric Field for PMN for 0.038 cm, and 0.050 cm (15 and 20 mil) Thick Samples and for PLZST 2/60/29/11 AFE-FE Material. Effective Dielectric Constants Corresponding to Linear Capacitance Approximation of Pulse Discharge Current Measurements are Indicated.

The small signal dielectric constant versus bias field is shown in Figure 13 for the PLZST 29/11 capacitor. In addition, the k vs. E graphs for 2 PMN discharge capacitors of different thickness are also shown. The k vs. E graphs were generated from polarization versus field characteristics. The vertical black lines in the graph indicate the field at which the linear capacitance equivalent, calculated from pulse discharge tests, occurred for the PMN materials. The field values for the 20 mil sample were not used in our final analysis because the inductance and resistance were slightly different than the final values for the HIDS design. The HIDS design was modified during the course of the project, after measurements on the 20 mil capacitor had already been performed. Figure 14 shows the

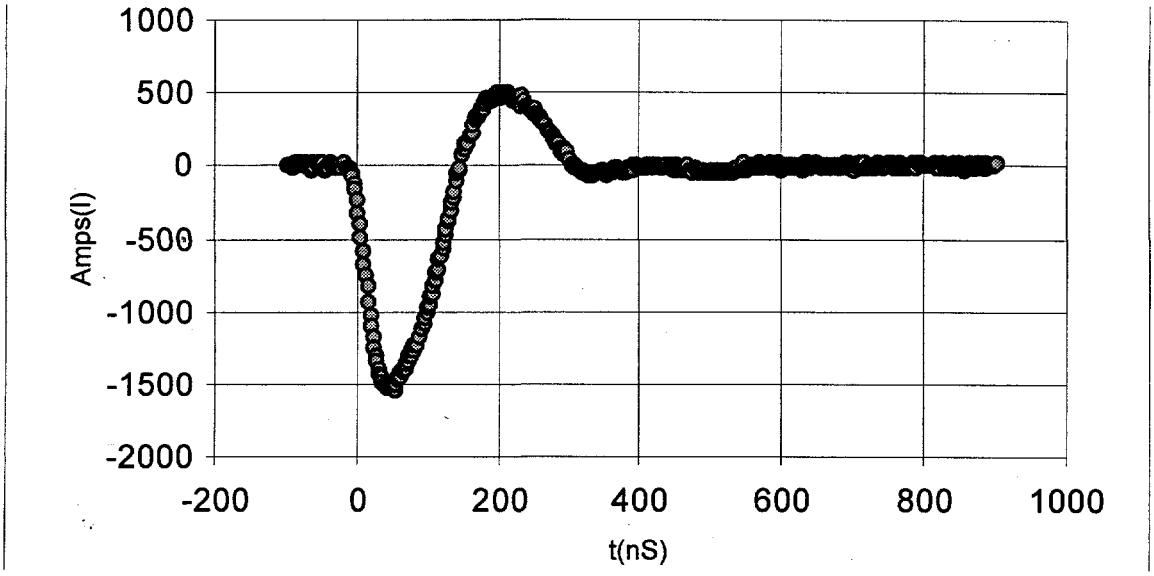

Figure 14. Pulse Discharge Current Versus Time for 0.015" Thick PMN Capacitor Charged to 1000 Volts.

pulse discharge current versus time for a 0.015" thick capacitor with 5 milliohm load resistance. A linear RLC circuit with parameters of 105 nF capacitance, 17.8 nH inductance and 0.284 ohms resistance fits the measured data very well. The added 0.23 ohms of resistance is not unusual for ceramic capacitors, such as $BaTiO_3$, in pulse discharge measurements. Combining the pulse discharge modeling with the capacitance versus field measurements on the 15 mil sample, indicates that the capacitance measured at approximately 12 kV/cm or 460 volts is most appropriate in evaluating capacitors for pulse discharge applications. The maximum capacitance for the AFE to FE material occurs at a field of approximately 14.5 kV/cm. From this data, the optimum thickness (T) to enhance peak current output for a single layer PLZST 29/11 capacitor charged to 1000 volts is 0.032 cm (0.013"), as shown in equation 5.

$$T = V / E = 460 \text{ volts} / 14{,}500 \text{ volts} / \text{cm} = 0.032 \text{ cm} \qquad (5)$$

Measurements of polarization vs. field for the four different PLZST compositions showed a monotonic change in the AFE-FE transition field with Sn:Ti ratio. The PLZST phase diagram [5] that we used to select our compositions is shown in Figure 12. As the titanium content in the PLZST increases, the material becomes closer in energy to the FE phase and thus requires a lower electric field to switch from the AFE phase to the FE phase. In the pulse discharge application, the capacitor will be charged to 1000V and discharged through an inductor and a resistor. Because the PLZST capacitor has a higher

dielectric constant at high fields than the PMN capacitor, the equivalent pulse discharge capacitance is 55% larger. Thus, with the appropriate design, a higher capacitance at higher voltage is achieved for the PLZST material as shown in figure 15. The single layer PLZST dielectric should give a peak current output of approximately 1750 amperes, which is 17% larger than that of the best PMN ceramics in our study.

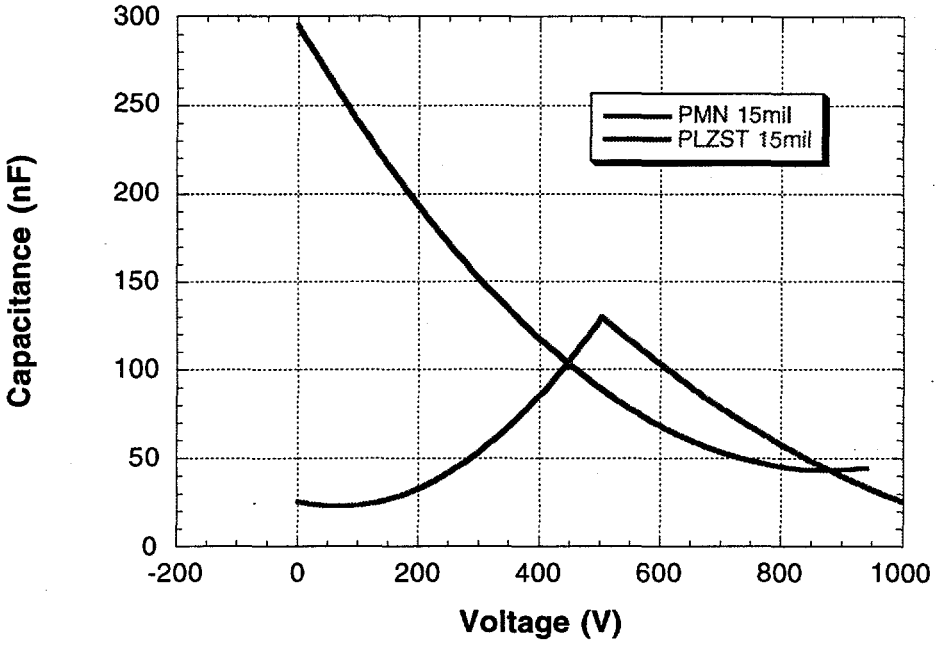

Figure 15. Capacitance Versus Voltage for 0.038 cm (15 mil) Thick PMN and PLZST 2/60/31/9 Ceramics.

There are two concerns with using the PLZST field enforced AFE to FE materials for HIDS type applications. The first issue is that the capacitor is required to discharge in the 30 to 70 nanosecond time frame. Because of the volume change (approximately 0.4%) associated with switching between FE and AFE states there is a great deal of mechanical stress generated within the sample during the pulse discharge test. When this volume change occurs in the nanosecond time frame, exceptionally high strain rates that lead to large localized heterogeneous stress intensities occur. These stresses may result in catastrophic mechanical fracture of the PLZST samples. Studies are underway to determine if high speed switching will limit this technology.

The second issue that needs to be addressed for using PLZST discharge capacitors under fireset conditions is that a high output current density needs to be maintained over a wide range of temperatures, typically -55°C to 74°C. The hysteresis loops taken for a range of temperatures including -60°C, -45°C, -35°C -30°C, -25°C, -10°C, 0°C, 5°C, and 25°C for the PLZST 60/31/9 ceramic (figure 16) show that the AFE to FE transition field and thus the peak capacitance changes dramatically with changing temperature.

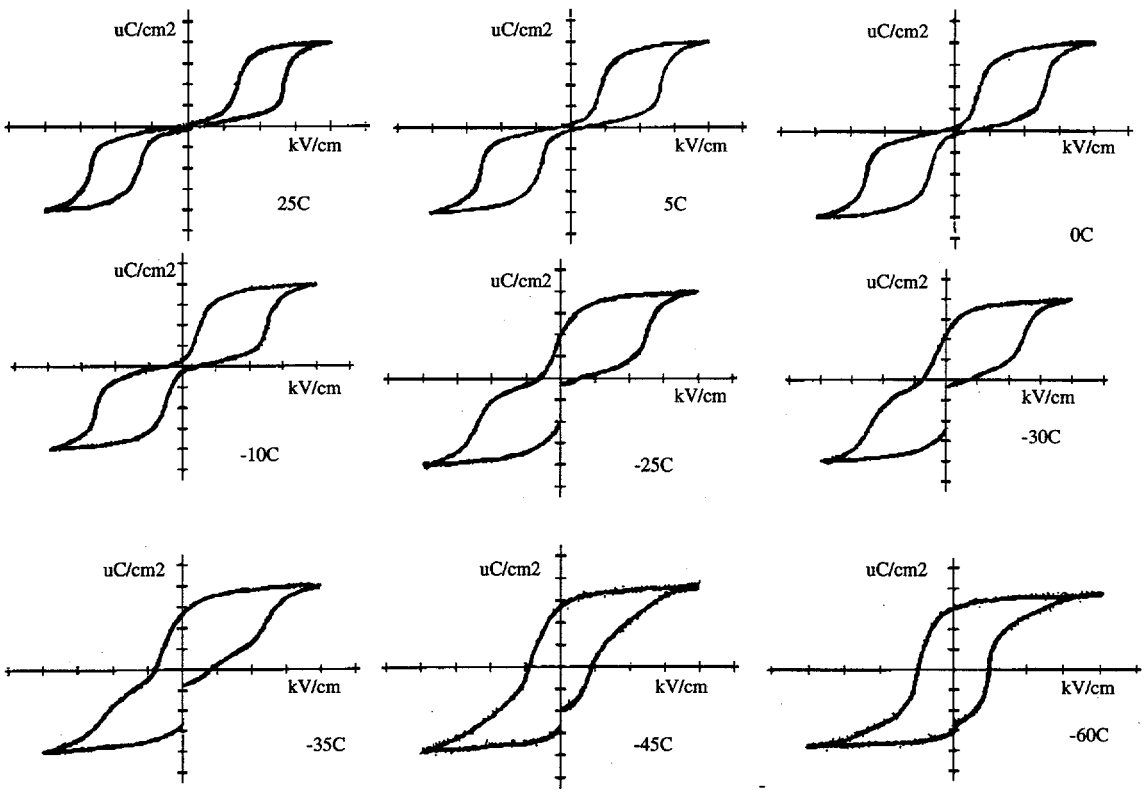

Figure 16. Polarization Versus Field Characteristics for PLZST 2/60/31/9 at the Following Temperatures: (a) 25°C, (b) 5°C, (c) 0°C, (d) -10°C (e) -25°C, (f) -35°C, (g) -45°C and (h) -60°C.

A major division on the polarization axis, labeled as $\mu C/cm^2$, is 6.5 $\mu C/cm^2$, while a major division on the electric field axis, labeled as kV/cm, is 20 kV/cm. At approximately -20°C, the maximum capacitance occurs at zero volts. At this temperature, the current output would be much too low for use in the HIDS. We estimate a lower temperature limit for fireset use of 0°C. Assuming the trend of increasing energy difference between the AFE and FE phase with increasing temperature there is the possibility that the AFE to FE transition voltage will exceed 1000V. For the HIDS application, the material would remain in the AFE state and have a dielectric constant of less than 2000. Peak discharge current densities would be approximately 1000 amperes. Improvements in temperature behavior can be made by compositional modifications, examples include lower Sn content or higher La content. However, developing AFE to FE transition materials that can function over the entire -55°C to 74°C temperature range is a challenge for the materials scientist.

The combination of being able to apply rather high fields and the high dielectric constants (greater than 10,000) at fields in excess of 100 kV/cm make these AFE to FE transition materials relatively unique for pulse discharge capacitor applications. For example, Figure 17 shows the polarization versus field characteristic (30 kV/cm and 6.5

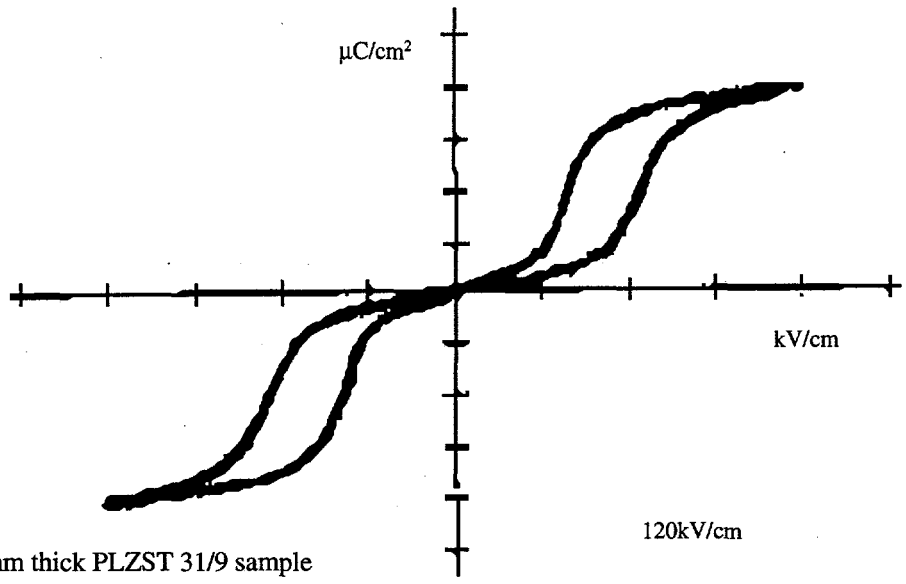

Figure 17. Polarization Versus Field Hysteresis Loop for PLZST 2/60/31/9 with 120 kV/cm Applied Field.

$\mu C/cm^2$ per division, for the field and polarization axes, respectively) for a PLZST 31/9 ceramic. The maximum applied field is 120 kV/cm. The material electrically broke down at 130 kV/cm; whereas, similarly prepared PMN ceramics have an electrical breakdown strength of 50 kV/cm. The ability of the AFE-FE PLZST material to withstand such high field strengths makes it a prime candidate for a multi-layer discharge capacitor. For example, a model discharge capacitor based on the PLZST 31/9 material would have a peak capacitance between 90 and 100 kV/cm. The capacitance that could be achieved in the same volume as that for the HIDS project was calculated to be 1.85μF. Our capacitor design consists of a capacitor that has five dielectric layers with each layer being 0.010 cm (4 mils) thick, for a total thickness of .020", which is the original HIDS thickness specification. The 1.85μF capacitance is a factor of 10 greater than the single layer PMN or a factor of 14 greater than single layer commercial X7R material[7]. Because dielectric constant decreases with field and saturates at a value less than 800 for both the PMN and $BaTiO_3$ materials, multilayer technology would be substantially less effective than for the AFE to FE materials. An effective capacitance of 1.85μF would provide a peak pulse discharge current output of 2700 amperes. This is almost twice the maximum peak current that is obtainable by the PMN material of the same volume.

Summary

We have fabricated single layer PLZST field enforced AFE to FE ceramics which have an effective dielectric constant for pulse discharge applications that is 55% greater than that of PMN based capacitors and over twice as great as $BaTiO_3$ based capacitors. Further, the PLZST materials have a high dielectric breakdown strength, which coupled with the high polarization once the FE phase is induced, make it possible to be fabricated in thin multilayers and still be able to meet HIDS volume and thickness requirements. We used RLC circuit analysis to demonstrate that a PLZST 2/62/30/9 ceramic five layer capacitor that has a total thickness of 0.051 cm should have ten times the capacitance and be able to generate more than twice the peak current output during discharge than that of a single layer PMN based ceramic of the same thickness. Unfortunately, there are two major issues that must be resolved for the AFE to FE PLZST technology to be used for Sandia's pulse discharge applications. The first is that its polarization versus field characteristics and thus equivalent capacitance vary substantially with a change in the temperature. For the present compositions studied, insufficient current output would be obtained for temperatures below 0°C. The second issue is that the PLZST materials must still be evaluated for high speed discharge testing.

References

1. P.A. Smith SAND97- (to be Published)
2. B.A. Tuttle, B.D. Hoover, W.R. Olson, D.M. Goy, R.A. Brooks, C.F. King, and P.A. Smith, Development of Lead Magnesium Niobate/ Lead Titanate Relaxor Pulse Discharge Capacitors for the Highly Integrated Detonator System, Sandia National Laboratories, Albuquerque NM SAND97- (to be Published)
3. M.D. Waugh, F.J. Toal, M-J. Pan, T.R. Shrout and C.A. Randall, Structure-Property Investigation for a Modified $PbHfO_3$ Composition for High Energy Storage, American Ceramic Society Meeting, Cincinnati , Ohio, May 6, 1997 paper SXIII-016-97 (1997).
4. G.H. Haertling, in private communications, 1997.
5. K. Merkowski, S-E. Park and S. Yoshiawa and L.E. Cross, Effect of Compositional Variations in the Lead Lanthanum Zirconate Stannate Titanate System on Electrical Properties, J. Am. Ceram. Soc., vol.79, 3297-304, 1997.
6. G. Love, Energy Storage in Ceramic Dielectrics, J. Amer. Ceram. Soc., vol. 73, 323-28, 1990.
7. W. Huebner, S.C. Zhang, M. Pennell, and X.M. Ding, High Energy Storage X7R Dielectrics, 99th Annual American Ceramic Society Meeting, Cincinnati , Ohio, May 6, paper SXI-048-97, 1997.
8. G.H. Haertling and C. Land, Hot-Pressed $(Pb,La)(Zr,Ti)O_3$ Ferroelectric Ceramics for Electrooptic Applications, J. Amer. Ceram. Soc., vol 54, No. 1, pp. 1-11, 1971.

Distribution:

Internal Distribution Only:

1	MS9018	Central Technical Files, 8940-2
5	MS 0899	Technical Library, 4916
1	0619	Review&Approval Desk, 12690
1	MS0311	G.E. Clark, 2671
1	MS0328	P.A. Smith, 2674
1	0328	A. Chappa, 2674
1	0328	J.A. Wilder, 2674
1	MS0333	T.J. Garino
1	MS0479	R.D. Holt
1	MS0523	R.A. Brooks, 1251
1	0523	C.F. King, 1251
1	0523	C.A. Hall, 1251
1	0523	J.O. Harris, 1251
1	0523	R.L. Edwards, 1251
1	MS0959	D.M. Goy, 1492
1	0959	R. H. Moore, 1492
1	0959	S.L. Lockwood, 1492
1	0959	F. Gerstle, 1492
1	0959	P. Yang, 1492
5	MS1405	B.A. Tuttle, 1812
1	1405	W.R. Olson, 1812
1	1405	C.L. Renschler, 1812
1	1405	J.A. Voigt, 1846
1	1405	D.L. Sipola, 1846
1	MS1411	D. Dimos, 1831